Desalination and Water Treatment
www.deswater.com

doi:10.5004/dwt.2017.20805

79 (2017) 188–195
June

Enhancement of hazardous pesticide uptake, ametryn using an environmentally friendly clay-based adsorbent

S.F.A. Shattar, N.A. Zakaria, K.Y. Foo*

River Engineering and Urban Drainage Research Centre (REDAC), Higher Institution Centre of Excellence (HiCoE), Engineering Campus, Universiti Sains Malaysia, Seri Ampangan, 14300 Nibong Tebal, Penang, Malaysia, email: ctfairosz89@yahoo.com.my (S.F.A. Shattar), redac01@usm.my (N.A. Zakaria), Tel. +6045996539, Fax +6045996926, email: k.y.foo@usm.my (K.Y.Foo)

Received 23 January 2017; Accepted 6 April 2017

ABSTRACT

To date, the indiscriminate discharge of pesticide contaminant into the water bodies is an imminent danger to the environment protection and natural ecosystems. Ametryn, a new generation of toxic pesticide with the annual application of 190 tonnes/year, has emerged to be a worldwide concern among the environmentalists. Considerable researches have been devoted to the developmental of the natural, non-conventional and functionalized adsorbents, which are abundantly available for the wide-scale treatment of toxic pesticides and their metabolites. In the present study, the feasibility of an acid modified montmorillonite (AM) for the adsorptive treatment of the hazardous ametryn was investigated. The physical, chemical and physicochemical behaviour of the prepared adsorbent was examined. Equilibrium data were simulated by the nonlinear Langmuir, Freundlich, Temkin and Redlich-Peterson isotherm models, while the adsorption kinetics were analysed by the pseudo-first order and pseudo-second order kinetic equations. The adsorption behaviour was well interpreted by the Langmuir isotherm model, with a monolayer adsorption capacity for ametryn of 207.71 mg/g. Kinetic data was fitted closely to the pseudo-second order kinetic equation, suggesting a chemisorption process. Thermodynamic parameters including the ΔG^{o}, ΔH^{o} and ΔS^{o} were evaluated. The adsorption process was found to be feasible, spontaneous and exothermic in nature. The findings illustrated the great applicability of AM as an ideal solution for the adsorptive treatment of the heavy polluted ametryn pesticide contaminated agricultural runoff.

Keywords: Acid modification; Adsorbent; Adsorption; Ametryn; Clay; Isotherm; Kinetic; Montmorillonite; Pesticide; Thermodynamic

1. Introduction

Ametryn, also known as N-ethyl-N-(1-methylethyl)-6-(methylthio)-1,3,5-triazine-2,4-diamine, has been recognized as the second generation of herbicide with selective action in the pre- and post-emergence agricultural crops. It is highly mobile, soluble with acute mutagenic, carcinogenic and teratogenic properties, and constitutes a source of hydro-geological contamination to the natural environment [1]. In view of the above matter, the urgency to the development of a low cost, efficient, easily operated, and new tertiary treatment technology is deeply required [2]. Among all, the establishment of a natural, novel and functionalized clay mineral, has prevailed to be a suitable candidate as a refining solution for the effective control of pesticide contaminants [3]. Montmorillonite, a smectite group of clay mineral characterized by an Al octahedral sheet, situated between two Si tetrahedral sheets, is featured by the high cation exchange capacity, large specific surface area and low cost of the parental rock bentonite [4]. In the mineral lattice, the isomorphous substitution of Al^{3+} with Fe^{2+} and Mg^{2+} in the octahedral sites, and Si^{4+} with Al^{3+} in the tetrahedral sites result in a net negative charge on the surface of montmorillonite. This negative charge could be balanced by the alkaline or alkaline earth metal ions located in the clay interlayer.

*Corresponding author.

These cations are exchangeable and strongly hydrated in the presence of water, leading to a high swelling capacity. Based on these properties, the structure of montmorillonite could be tailored by several modification techniques, including acid activation, ion exchange, and pillaring processes [5].

In particular, acid activation has been proposed to be one of the simplest, and most efficient route of modification selection [6]. During this process, the interlayer cations are replaced by protons, with partial dissolution of octahedral and tetrahedral sheets. Acid treatment also dissolves a series of impurities, enlarges the edges of the platelets, and significantly improves the specific surface area and pore diameter, resulting in the generation of new acid sites over the surface to create an amorphous, porous, protonated and hydrated silica, with a three dimensional cross-linked structure [7]. These transformations would promote important alteration in the surface acidity [8], and is a key strategic step for the practical improvement on the adsorption capacity of montmorillonite. In the present paper, we reported the adsorption of a basic pesticide, ametryn onto the hydrochloric acid treated montmorillonite (AM). The influence of initial concentrations, contact time and solution pH on the treatment process was examined. The adsorptions modelling, kinetic and thermodynamic were presented.

2. Materials and methods

2.1. Adsorbate

Ametryn, also known as N_2-ethyl-N_4-isopropyl-6-methylthio-1,3,5-triazine-2,4-diamine, was chosen as the model herbicide in this work. It is available with the purity of >99% from Sigma-Aldrich. The selected physicochemical properties of ametryn are listed in Table 1. The standard stock solution was prepared by dissolving 150 mg of adsorbate in 1 L of 0.01 mol/L of $CaCl_2$ solution. Working solutions were prepared by a series of successive dilutions.

2.2. Adsorbent

Montmorillonite, acquired from Sigma-Aldrich was selected as the raw material in this study. The modification process was carried out by mixing the montmorillonite with 50 mL of hydrochloric acid (HCl) solution at a pre-determined concentration of 2.0 M at 75°C, with the modification ratio (acid:clay) of 1:4. The modification process was terminated with the addition of a large amount of double-deionized water. The acidified montmorillonite was washed several times with double-deionized water until the Cl^- ion was undetectable in the supernatant solution using 0.1 M of silver acetate solution. The newly prepared adsorbent (AM) was dried at 60°C for 24 h, and stored in a desiccator for further use.

Table 1
Selected physicochemical properties of ametryn

Properties	Description
Chemical name	N_2-ethyl-N_4-isopropyl-6-methylthio-1,3,5-triazine-2,4-diamine
Chemical formula	$C_9H_{17}N_5S$
Molecular weight (g/mole)	227.33
pK_a	4.0
Log K_{ow}	3.07
Deff[3]/nm	1.12
Water solubility (mg/L)	185
Dipole moment[4]/Debye	3.51

2.3. Adsorption equilibrium studies

The batch adsorption studies were conducted in a set of 250 mL conical flask containing 200 mg of AM and 200 mL of ametryn solution within the concentration range of 25–150 mg/L. The mixtures were placed in a reciprocating thermostatic water bath shaker with an agitation speed of 120 rpm till the equilibrium was achieved. The supernatant solutions were filtered using a syringe filter to reduce the interference of clay nano-particles, and the concentration was determined spectrophotometrically using a UV-spectrophotometer (Shimadzu-1800) at the optimum wavelength of 224 nm. The adsorptive uptake of ametryn was computed from the difference between the initial and final/equilibrium concentrations derived as:

$$q_e = \frac{(C_0 - C_e)V}{W} \quad (1)$$

where q_e (mg/g) is the amount of ametryn adsorbed/weight of adsorbent at the equilibrium, while C_0 and C_e represent the initial and equilibrium concentrations of ametryn solution (mg/L), respectively. V(mL) is the volume of the solution, and W(g) is the dry weight of AM. The effect of solution pH on the adsorption process was performed in 100 mg/L of ametryn solution within the pH range of 2–12. The solution pH was adjusted using the 0.01 M of hydrochloric acid (HCl) or sodium hydroxide (NaOH) solution, and measured using a pH meter (Accumet XL200, Fischer Scientific). The experiments were repeated in three replications.

2.4. Batch kinetic studies

The procedures of kinetic experiments were identical to those of equilibrium tests, where the aqueous solutions were taken at preset time intervals, and the concentrations of ametryn were similarly measured. The adsorptive uptake of ametryn at time t, q_t (mg/g), was calculated by:

$$q_t = \frac{(C_0 - C_t)V}{W} \quad (2)$$

where q_t is defined as the adsorptive uptake of the ametryn at time (t), and C_t (mg/L) is the liquid-phase concentration of ametryn at time t.

2.5. Characterization of montmorillonite

The pore structural analysis was characterized by nitrogen adsorption at 77 K with an accelerated surface area and porosimetry system (Micromeritics ASAP 2020). The specific surface area was calculated by the Brunauer-Emmett-Teller (BET) equation; the total pore volume was evaluated by converting the adsorption volume of nitrogen at relative pressure of 0.95 to equivalent liquid volume of the adsorbate, while the micropore volume, micropore surface area and external surface area were deduced using the *t*-plot method. The surface morphology was examined using a scanning electron microscopy (SEM) (Zeiss Supra 35VP). The powdered sample was fixed to 10 mm of metal mounts using a carbon tape, and spit coated with gold under vacuum in an argon atmosphere. The Fourier Transform Infrared (FTIR) spectroscopy was performed using a Perkin-Elmer FTIR spectrophotometer with a smart endurance single bounce diamond ATR cell. Spectrum over the range of 4000–400 cm^{-1} was obtained by the co-addition of 64 scans, with the wave resolution of 4 cm^{-1} and a mirror velocity of 0.6329 cm/s.

3. Results and discussion

3.1. Textural and surface characterization

The examination of the textural characteristics of the raw montmorillonite and AM were evaluated from the scanning electron micrographs, as illustrated in Fig. 1. Generally, the raw of montmorillonite (Fig. 1a) appears to be relatively smooth with face-to-edge contacts between the particles, covered by small and well separated particles, as reported by Bianchi et al. [9] and Zhao et al. [6]. However, the acidified montmorillonite (AM) displays a ragged, highly porous and well develop cavities, governed by the partial leaching of Mg^{2+} or Al^{3+} cations from the 2:1 layers during the activation stage. The partially disaggregation of the original montmorillonite structure during acid treatment, resulting from the collapse of the interlayer, would generate a series of small aggregates of nanoparticles, with a distinct porous natural surface. Similar behaviour has been described by Novaković et al. [10] in the acidification of Serbian smectite clays.

Nitrogen adsorption-desorption curve provides qualitative information on the adsorption mechanism and porous structure of the carbonaceous adsorbents [11]. The surface physical parameters obtained from the nitrogen adsorption isotherm are listed in Table 2. The BET surface area, Langmuir surface area and total pore volume of the original montmorillonite was 162.23 m^2/g, 206.45 m^2/g, and 0.271 cm^3/g, respectively, with an average pore size of 65.74 Å. Conversely, the acid modified AM display the BET surface area, Langmuir surface area, and total pore volume of 245.64 m^2/g, 306.16 m^2/g, and 0.340 cm^3/g, respectively, implying significant pore development, and widening of the existing pores during the activation stage.

The reference band assignments of AM are given in Table 3. The obtained FTIR spectrum of AM exhibits intensive peaks at 1047, 797, 526, and 470 cm^{-1}, attributed

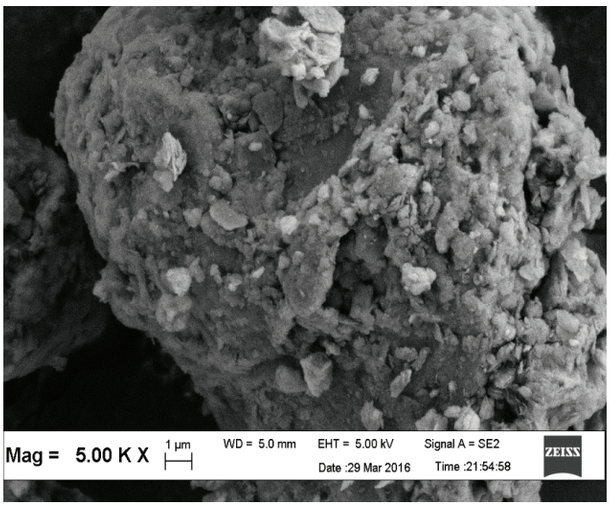

(a)

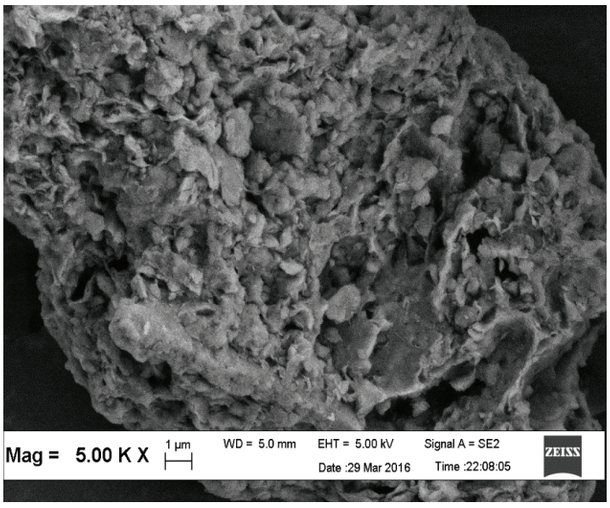

(b)

Fig. 1. SEM micrographs of the (a) raw montmorillonite and (b) AM .

Table 2
Surface physical parameters for montmorillonite and AM

Properties	Montmorillonite	AM
BET surface area (m^2/g)	162.23	245.64
Micropore surface area (m^2/g)	38.48	27.76
External surface area (m^2/g)	126.31	217.88
Langmuir surface area (m^2/g)	206.45	306.16
Total pore volume (cm^3/g)	0.2708	0.3397
Micropore volume (cm^3/g)	0.0168	0.0124
Mesopore volume (cm^3/g)	0.2540	0.3273
Average pore size(Å)	65.74	55.31

Table 3
FTIR band assignments of AM

Wavelength (cm^{-1})		Assignment
Montmorillonite	AM	
3617	3617	–OH stretching vibrations
3431	3435	–OH stretching, hydration
2928	–	$–CH_2$ asymmetric stretching group
1634	1634	–OH bending, hydration
1047	1043	Si–O streching in and out of the plan
797	797	Al–Mg–OH bending
694	694	–OH bending
526	526	Si–O–Al deformation vibration
470	471	Si–O–Si bending

to the Si–O stretching vibrations, OH bending band (AlMgOH), Si–O–Al deformation vibration (octahedral Al), and Si–O–Si bending vibrations, respectively. A comparison of the FTIR spectra demonstrated alteration of the intensities of the adsorption bands, at 1047 and 2928 cm^{-1}, indication of the structural changes of the clay minerals, and formation of the amorphous silica phase during acid modification. During the process, the acid attacking protons would penetrate into the clay mineral layers, and attack the structural OH groups, resulting in the dehydroxylation process, connected with the successive release of central atoms from octahedral, and the removal of Al from the tetrahedral sheets. During this time, a gradual transformation of the layered tetrahedral sheet to a three-dimensional framework would proceed [12].

3.2. Effect of initial concentrations, contact time and solution pH on the adsorption equilibrium

Generally, the adsorptive uptake and adsorptive removal of ametryn increased with prolonging the contact time. The curve adsorption uptake, q_t as a function of time, t at the initial concentration of 25–150 mg/L is depicted in Fig. 2. Initially, the amount of ametryn adsorbed onto the AM surface increased rapidly, and with a lapse of time, the process slowed down and reached to a plateau. The initial concentration provides an essential driving force to overcome the mass transfer resistance between the aqueous phase and the solid medium [13]. In the present study, the adsorption equilibrium, q_e increased from 23.36 to 128.46 mg/g with an increase of initial concentration from 25 to 150 mg/L. Conversely, there was a reverse relationship between the equilibrium concentrations with the initial ametryn concentrations. The equilibrium concentration, C_e obtained at 25, 50, 75, 100, 125 and 150 mg/L, was 1.64, 3.72, 6.71, 9.91, 14.71 and 21.54 mg/L, respectively, indicating high percent removal of ametryn, even at high initial concentrations.

Solution pH could affect the adsorption process by regulating the adsorbent surface charge as well as degree of ionization of adsorbates present in the solution [14]. The adsorption behavior of ametryn over a broad pH range of 2–12 is shown in Fig. 3. It was found that decreasing

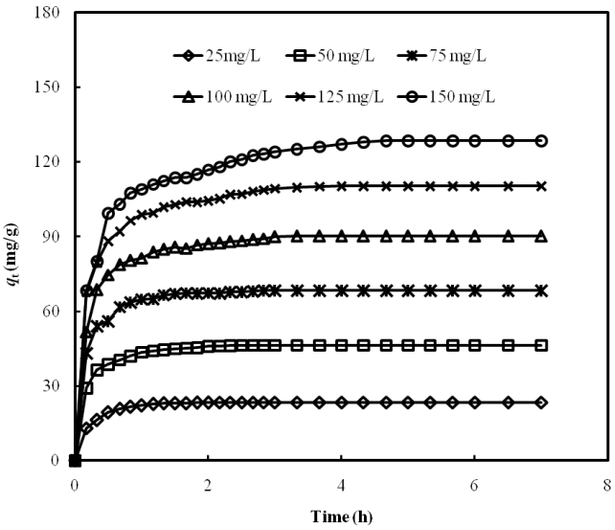

Fig. 2. Effect of initial concentrations and contact time on the adsorptive uptake of ametryn onto AM at 30°C.

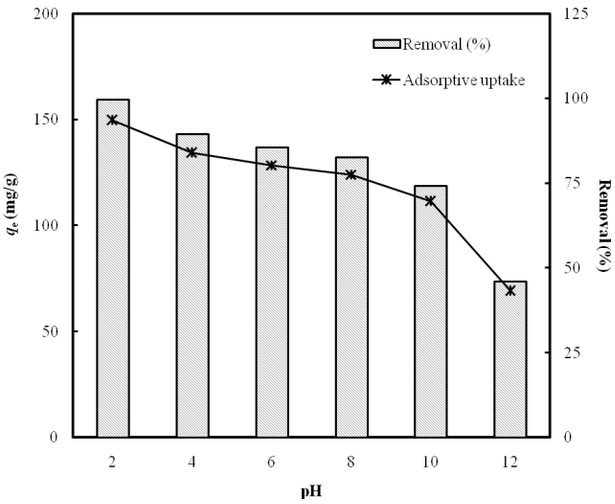

Fig. 3. Effect of solution pH on the adsorptive uptake and adsorptive removal of ametryn onto AM at 30°C

solution pH serves to increase the adsorption capacity, with a significant enhancement as the pH decreased from 6 to 2. Solution pH would influence the degree of equilibrium of the adsorbate,with the maximum sorption at a pH in the vicinity of acid dissociation constant, pK_a of the weakly basic ametryn. Ametryn, characterized by the pK_a of 4.1 would get protonated as the pH decreased, and the resulting cations would be adsorbed to the negatively clay particles. Reduced protonation of ametryn at higher solution pH is responsible to the lower adsorption capacity of ametryn onto AM. At the pH above the values of pK_a, ametryn would exist predominantly in the anionic forms, and as the solution pH increased, the extent of dissociation of these molecules would increase and they turned negatively charged. This resulted to a higher electrostatic repulsion, or dispersion between the adsorbent and adsorbate molecules

in the studied pH range. Similar phenomenon was recorded by Ahmad et al. [15] in the adsorption of ametryn onto the natural soil media.

3.3. Adsorption isotherm

Adsorption isotherm describes the distribution of solutes molecules between the liquid and the solid phases when the adsorption process reaches to the equilibrium [16]. The analysis of adsorption isotherm is an important step for the identification of well suitable model that could be applied for design purposes [17], and critical in the optimization uses of the adsorbents. In the present study, four isotherm models, Langmuir, Freundlich, Temkin and Redlich-Peterson isotherm models were established. The applicability of the isotherm models was carried out by judging the correlation coefficients, R^2 values, defined as:

$$R^2 = \frac{(q_{e,meas} - \overline{q_{e,calc}})^2}{\sum (q_{e,meas} - \overline{q_{e,calc}})^2 + (q_{e,\,meas} - q_{e,calc})^2} \quad (3)$$

where $q_{e,meas}$, $q_{e,calc}$ and $\overline{q_{e,\mathrm{calc}}}$ are the measured, calculated and average mean adsorbate concentration (mg/g), respectively. Langmuir isotherm equation [18] is valid for monolayer adsorption on a surface, with a finite number of identical sites expressed as:

$$q_e = \frac{Q_0 K_L C_e}{1 + K_L C_e} \quad (4)$$

where Q_0 (mg/g) is the maximum amount of adsorbate per unit weight of adsorbent to form a complete monolayer onto the surface, and K_L (L/mg) is the Langmuir isotherm constant related to the affinity of the binding sites.

Freundlich isotherm model assumes heterogeneous surface energy, in which the energy would vary as a function of the surface coverage. According to the model, the stronger binding sites would be occupied first, and the binding strength decreases with increasing the degree of the site occupation [19]. The well-known nonlinear form of Freundlich isotherm model is given by:

$$q_e = K_F C_e^{1/n} \quad (5)$$

where K_F and n are the Freundlich isotherm constants, with n provides an indication on the favourably of the adsorption process, and K_F (mg/g (L/mg)$^{1/n}$) is the adsorption capacity of the adsorbent. K_F can be defined as the adsorption or distribution coefficient, and represents the quantity of ametryn adsorbed onto AM for a unit of equilibrium concentration. The slope of $1/n$ ranging between 0 and 1 is a measure of the adsorption intensity or surface heterogeneity, becoming more heterogeneous as its value gets closer to zero. A value for $1/n$ below one indicates a normal Langmuir isotherm, while $1/n$ above one is indicative of the cooperative adsorption.

Temkin isotherm [20] contains a factor that explicitly takes into the account related to adsorbent-adsorbate interactions. According to the model, the heat of adsorption of all molecules in the layer would decrease linearly with coverage due to the adsorbent-adsorbate interactions. The adsorption is characterized by a uniform distribution of binding energy, up to some maximum binding energy. The Temkin isotherm model is expressed by:

$$q_e = \frac{RT}{b_T} \ln(AC_e) \quad (6)$$

where $B = RT/b_T$, is the Temkin isotherm constant, A (L/g) is the equilibrium binding constant corresponding to the maximum binding energy, R (8.314 J/mole K) is the universal gas constant, b_T (J/mole) is the Temkin isotherm constant related to heat of adsorption and T (K) is the absolute temperature.

Redlich-Peterson isotherm [21] is a hybrid isotherm featuring both Langmuir and Freundlich isotherms, which incorporates three parameters into an empirical equation derived as:

$$q_e = \frac{K_R C_e}{(1 + \alpha_R C_e^g)} \quad (7)$$

where K_R (L/g) and α_R (1/mg) g are Redlich-Peterson isotherm constants, and g is the isotherm exponent. The model has a linear dependence on concentration in the numerator, and an exponential function in the denominator to represent adsorption equilibrium over a wide concentration range. In the limit, it approaches Freundlich isotherm model at high concentration, and in accordance to the low concentration limit of the ideal Langmuir condition.

The correlation coefficient, R^2 values and the isotherm parameters at the adsorption temperatures of 30, 40 and 50°C are summarized in Table 4. For all of the tested temperatures, the highest R^2 value of 0.998 to 0.999 reported in the Table 4 showed a strong positive evidence that the

Table 4
Isotherm parameters for the adsorption of ametryn onto AM at 30, 40 and 50 °C

Isotherms	Constants		
	30°C	40°C	50°C
Langmuir			
Q_0 (mg/g)	207.71	199.35	190.41
K_L (L/mg)	0.076	0.0574	0.0373
R^2	0.999	0.999	0.998
Freundlich			
K_F (mg/g)·(L/mg)$^{1/n}$	22.068	17.721	12.584
n	1.706	1.690	1.645
R^2	0.983	0.984	0.981
Temkin			
A (L/g)	0.915	0.674	0.441
B	41.559	40.284	38.157
R^2	0.977	0.981	0.976
Redlich-Peterson			
A_g (1/mg)^2	0.071	0.053	0.022
K_R (L/g)	15.571	11.263	6.607
g	1.01	1.02	1.12
R^2	0.998	0.999	0.998

adsorption of ametryn onto AM was best described by the Langmuir isotherm model. The suitability of the Langmuir isotherm to fit the data was ascertained by the exponent value of the Redlich-Peterson isotherm model that provided the *g* value approximate to unity, resulted to the original Langmuir equation. The fitting of the adsorption data to the Langmuir adsorption isotherm revealed uniform adsorption and strong ametryn-adsorbent interactions over the surfaces of AM, suggested that the adsorption was limited to the monolayer coverage, and the surface was energetically homogenous. Table 5 lists a comparison of the maximum monolayer adsorption capacity of ametryn onto various adsorbents. AM prepared in this work showed relatively high adsorption capacity of 207.71 mg/g, as compared to some previous works as reported in the literature.

3.4. Kinetic modelling

Adsorption kinetic provides a valuable insight into the controlling mechanism of the adsorption process, which in turn governs mass transfer and the residence time [27].The experimental data of ametryn adsorption onto AM at different time intervals were simulated by the pseudo-first order and pseudo-second order kinetic models, using the plots $\ln(q_e - q_t)$ against t, and t/q_t versus t, respectively. When the adsorption is preceded by diffusion through a boundary, the kinetic in most systems follow the pseudo-first order kinetic model. The model given by Lagergren and Svenska [28] is defined as:

$$\ln(q_e - q_t) = \ln q_e - \frac{k_1}{2.303} t \tag{8}$$

where k_1 (1/h) is the pseudo-first order kinetic rate constant. Contrary to the other models, pseudo-second order kinetic equation [29] predicts the behaviour over the whole time of adsorption, with chemisorption being the rate controlling step given by:

$$\frac{t}{q_t} = \frac{t}{q_e} + \frac{1}{k_2 q_e^2} \tag{9}$$

where k_2 (g/mg h) is the pseudo-second order kinetic rate constant. The suitability of the kinetic model to describe the adsorption process was verified by the correlation coefficient, R^2, and further validated by the normalized standard deviation, Δq (%) derived as:

$$\Delta q\ (\%) = 100\sqrt{\frac{\sum \left|(q_{e,\exp} - q_{e,cal}) / q_{e,\exp}\right|^2}{n-1}} \tag{10}$$

where n is the number of data points, and $q_{e,\exp}$ (mg/g) and $q_{e,\text{cal}}$ (mg/g) are the experimental and calculated adsorption capacities, respectively.

From Table 6, the experimental data showed good agreement with the pseudo-second order kinetic equation, with the lowest normalized standard deviation, Δq (%) values which ranged between 0.20% and 11.77%. Moreover, the correlation coefficient, R^2 values for the pseudo-second order kinetic model were higher for all ametryn concentrations. This suggested that the adsorption system followed the pseudo-second order model, based on the assumption that the rate-limiting step may be chemisorption, which involves valency forces through electrons sharing between AM and the ametryn cations.

3.5. Adsorption thermodynamic

Thermodynamic parameters including the Gibbs free energy change ($\Delta G°$), enthalpy change ($\Delta H°$) and entropy change ($\Delta S°$) are among the most critical aspect in predicting the stability of an adsorption system [30]. The concept of thermodynamic assumes that in an isolated system where energy cannot be gained or lost, entropy change is the driving force. The value of $\Delta H°$ and $\Delta S°$ were computed following the equations:

$$\ln K_d = \frac{\Delta S°}{R} - \frac{\Delta H°}{RT} \tag{11}$$

where K_d is the distribution coefficient that can be determined by:

$$K_d = \frac{C_{Ae}}{C_e} \tag{12}$$

where C_{Ae} (mg/L) is the amount of ametryn adsorbed on the solid phase at equilibrium, and C_e (mg/L) is the equilibrium concentration of ametryn. The values of $\Delta H°$ and $\Delta S°$ were calculated from the slope and intercept of the plot $\ln K_d$ versus $1/T$, and $\Delta G°$could be estimated using the relation:

$$\Delta G° = -RT \ln K_d \tag{13}$$

The calculated values of $\Delta H°$, $\Delta S°$ and $\Delta G°$ are listed in Table 7. The positive value of $\Delta S°$(82.630 J/mole*K*) revealed the affinity of AM, and increasing randomness at the solid-solution interface during the fixation of ametryn onto the active sites of AM. Negative $\Delta G°$ of –4.498, –3.862 and –2.837kJ/mole at 30, 40 and 50°C, respectively dictated spontaneous nature of the adsorption process, while negative $\Delta H°$ (–29.595 kJ/mole) indicated exothermic of the adsorption process. The findings of the negative $\Delta H°$ was consistent with the results obtained, where increasing temperature denoted a decrease of the monolayer adsorption capacity for ametryn from 207.71 to 190.41 mg/g at the temperature range of 30–50°C. This exothermic process

Table 5
A comparison of the monolayer adsorption capacities of ametryn onto different adsorbents

Adsorbent	Adsorption capacity (mg/g)	Reference
AM	207.71	Present study
Kaolin	1.82	[22]
Activated carbon-cloth (spectracarb 2225)	354.61	[23]
Commercial activated carbon	230.00	[24]
Chalk	1.55	[25]
Soil	0.05–0.13	[26]

Table 6
Adsorption kinetic parameters for the adsorption of ametryn onto AM at 30 °C

C_0 (mg/L)	$q_{e,exp}$ (mg/g)	Pseudo-first-order				Pseudo-second-order			
		$q_{e,cal}$ (mg/g)	k_1 (1/h)	R^2	Δq (%)	$q_{e,cal}$ (mg/g)	k_2 (g/mg h)	R^2	Δq (%)
25	23.36	18.79	6.401	0.9828	19.56	26.11	0.210	0.9989	11.77
50	46.28	31.13	5.776	0.9379	32.74	47.85	0.182	0.9992	3.39
75	68.29	47.99	6.423	0.9552	29.73	72.46	0.112	0.9982	6.11
100	90.10	59.72	5.105	0.8978	33.72	91.74	0.091	0.9992	1.82
125	110.30	74.09	4.717	0.9131	32.83	109.89	0.075	0.9992	0.37
150	128.46	93.64	4.163	0.9084	27.11	128.21	0.047	0.9961	0.20

Table 7
Thermodynamic parameters for the adsorption of ametryn onto AM

$\Delta G°$ (kJ/mole)			$\Delta H°$ (kJ/mole)	$\Delta S°$ (J/mole$K$)
30°C	40°C	50°C		
–4.498	–3.862	–2.837	–29.595	82.630

was attributed to the weakening of the adsorptive forces between the binding sites and the ametryn species, and between the adjacent ametryn molecules on the adsorbed phase. Additionally, higher temperature may enhance the solubility and desorption rate of ametryn, hence the solute molecules were more difficult to be adsorbed. This phenomenon has also been observed in the adsorption of pendimethalium herbicide onto natural clay heated at 550°C [31], and further supported by El Bakouri et al. [32] which reported that, the lower removal efficiency at the higher operating temperatures could be ascribed to the greater solubility of endosulfan, which reduced the affinity of endosulfan sulphate onto the surface of the biosorbents.

4. Conclusion

The potential of the acid modified montmorillonite as a promising alternative for the effective treatment of ametryn contaminant has been attempted. Experimental data revealed that low contact time of lesser than 4 h was sufficient for the adsorption process to reach to the equilibrium stage. The adsorption equilibrium was best represented by the Langmuir isotherm model, with a maximum monolayer adsorption capacity of 207.71 mg/g. Kinetic data were best confronted to the pseudo-second order kinetic model, suggesting chemisorption was the rate limiting step. The resulting thermodynamic parameters suggested that the sorption process was spontaneous and exothermic in nature. These findings outlined the newly developed AM as an excellent adsorbent for the on-site remediation of ametryn contaminated wastewater.

Acknowledgement

The authors acknowledge the financial support provided by the Ministry of Higher Education of Malaysia and Universiti Sains Malaysia under the Research University (Project No. 1001/PREDAC/814272) and FRGS (Project No. 304/PREDAC/6171157) grant schemes.

References

[1] C.R. Silva, T.F. Gomes, G.C.R.M. Andrade, S.H. Monteiro, A.C.R. Dias, E.A.G. Zagatto, V.L. Tornisielo, Banana peel as an adsorbent for removing atrazine and ametryne from waters, J. Agric. Food Chem., 61 (2013) 2358–2363.
[2] Z. Qin, S. Liu, S.-X. Liang, Q. Kang, J. Wang, C. Zhao, Advanced treatment of pharmaceutical wastewater with combined micro-electrolysis, Fenton oxidation, and coagulation sedimentation method, Desal. Water Treat., 57 (2016) 25369–25378.
[3] H. Herbache, A. Ramdani, A. Maghni, Z. Taleb, S. Taleb, E. Morallon, R. Brahmi, Removal of o-cresol from aqueous solution using Algerian Na-clay as adsorbent, Desal. Water Treat., 57 (2016) 20511–20519.
[4] A. Nadali, M. Khoobi, R. Nabizadeh, S. Naseri, A.H. Mahvi, Performance evaluation of montmorillonite and modified montmorillonite by polyethyleneimine in removing arsenic from water resources, Desal. Water Treat., 57 (2016) 21645–21653.
[5] S.F.A. Shattar, N.A. Zakaria, K.Y. Foo, Feasibility of montmorillonite-assisted adsorption process for the effective treatment of organo-pesticides, Desal. Water Treat., 57 (2016) 13645–13677.
[6] Y.-H. Zhao, F. Ma, K. Tang, Preparation of acid-activated montmorillonite and its application, Mar. Georesour. Geotechnol., 34 (2016) 741–746.
[7] Z. Jukui, Y. Jun, S. Lei, Preparation and characterization of a novel multi-component composite biological filler, Desal. Water Treat., 57 (2016) 9635–9643.
[8] F. Franco, M. Pozo, J.A. Cecilia, M. Benítez-Guerrero, M. Lorente, Effectiveness of microwave assisted acid treatment on dioctahedral and trioctahedral smectites. The influence of octahedral composition, Appl. Clay Sci., 120 (2016) 70–80.
[9] A.E. Bianchi, M. Fernández, M. Pantanetti, R. Viña, I. Torriani, R.M.T. Sánchez, G. Punte, ODTMA$^+$ and HDTMA$^+$ organo-montmorillonites characterization: New insight by WAXS, SAXS and surface charge, Appl. Clay Sci., 83–84 (2013) 280–285.
[10] T. Novaković, L. Rožić, S. Petrović, A. Rosić, Synthesis and characterization of acid-activated Serbian smectite clays obtained by statistically designed experiments, Chem. Eng. J., 137 (2008) 436–442.
[11] K.Y. Foo, B.H. Hameed, A cost effective method for regeneration of durian shell and jackfruit peel activated carbons by microwave irradiation, Chem. Eng. J., 193 (2012) 404–409.
[12] J. Madejová, FTIR technique in clay mineral studies, Vib. Spectrosc., 31 (2003) 1–10.
[13] K.Y. Foo, B.H. Hameed, An overview of dye removal via activated carbon adsorption process, Desal. Water Treat., 19 (2010) 255–274.

[14] T.-H. Pham, B.-K. Lee, J. Kim, C.-H. Lee, Improved removal of Cd (II) from aqueous solution by synthesized nanozeolite, Desal. Water Treat., 57 (2016) 29457–29466.
[15] R. Ahmad, R.S. Kookana, A.M. Alston, Sorption of ametryn and imazethapyr in twenty-five soils from Pakistan and Australia, J. Environ. Sci. Health., Part B, 36 (2001) 143–160.
[16] K.Y. Foo, B.H. Hameed, A rapid regeneration of methylene blue dye-loaded activated carbons with microwave heating, J. Anal. Appl. Pyrolysis, 98 (2012) 123–128.
[17] K.Y. Foo, B.H. Hameed, Insights into the modeling of adsorption isotherm systems, Chem. Eng. J., 156 (2010) 2–10.
[18] I. Langmuir, The Adsorption of gases on plane surfaces of glass, Mica and Platinum, J. Am. Chem. Soc., 40 (1918) 1361–1403.
[19] H.M.F. Freundlich, Over the adsorption in solution, J. Phys. Chem., 57 (1906) 385–471.
[20] M.J. Temkin, V. Pyzhev, Kinetics of ammonia synthesis on promoted iron catalysts, Acta Physicochim URSS, 12 (1940) 217–222.
[21] O. Redlich, D.L. Peterson, A useful adsorption isotherm, J. Phys. Chem., 63 (1959) 1024–1026.
[22] Q. Wang, A.T. Lemley, Reduced adsorption of ametryn in clay, humic acid, and soil by interaction with ferric ion under fenton treatment conditions, J. Environ. Sci. Health., Part B, 41 (2006) 223–236.
[23] E. Ayranci, N. Hoda, Adsorption kinetics and isotherms of pesticides onto activated carbon-cloth, Chemosphere, 60 (2005) 1600–1607.
[24] Y. Yang, Y. Chun, G. Shang, M. Huang, pH-dependence of pesticide adsorption by wheat-residue-derived black carbon, Langmuir, 20 (2004) 6736–6741.
[25] A. Wefer-Roehl, E.R. Graber, M.D. Borisover, E. Adar, R. Nativ, Z. Ronen, Sorption of organic contaminants in a fractured chalk formation, Chemosphere, 44 (2001) 1121–1130.
[26] C. Sluszny, E.R. Graber, Z. Gerstl, Sorption of s-triazine herbicides in organic matter amended soils: Fresh and incubated systems, Water Air Soil Pollut., 115 (1999) 395–410.
[27] K.Y. Foo, Value-added utilization of maize cobs waste as an environmental friendly solution for the innovative treatment of carbofuran, Process Saf. Environ. Prot., 100 (2016) 295–304.
[28] S. Lagergren, B.K. Svenska, Zur theorie der sogenannten adsorption geloester stoffe, Veternskapsakad Handlingar, 24 (1898) 1–39.
[29] Y.S. Ho, G. McKay, The Kinetics of sorption of basic dyes from aqueous solution by Sphagnum moss peat, Can. J. Chem. Eng., 76 (1998) 822–827.
[30] K.Y. Foo, L.K. Lee, B.H. Hameed, Preparation of banana frond activated carbon by microwave induced activation for the removal of boron and total iron from landfill leachate, Chem. Eng. J., 223 (2013) 604–610.
[31] M.S. El-Geundi, T.E. Farrag, H.M.A. El-Ghany, Adsorption equilibrium of a herbicide (pendimethalin) onto natural clay, Adsorpt. Sci. Technol., 23 (2005) 437–453.
[32] H. El Bakouri, J. Morillo, J. Usero, A. Ouassini, Natural attenuation of pesticide water contamination by using ecological adsorbents: Application for chlorinated pesticides included in European Water Framework Directive, J. Hydrol., 364 (2009) 175–181.